Using Tipifarnib to prevent resistance to targeted therapies in oncogene-addicted tumors

Célia Delahaye[1*], Sarah Figarol[1*], Mathylda Brachais[1], Rémi Gence[1], Aurélia Doussine[1], Estelle Clermont[1,2,3], Jacques Colinge[5], Jean-Philippe Villemin[5], Antonio Maraver[5], Irene Ferrer[6], Luis Paz-Ares[6], Luc Friboulet[7], Estelle Clermont[1,2,3], Anne Casanova[1,2,3], Anne Pradines[1,2,3], Julien Mazières[1,2,4], Gilles Favre[1,2,3#], Olivier Calvayrac[1#]

[1]Inserm, CNRS, Centre de Recherches en Cancérologie de Toulouse, Université de Toulouse, Université Toulouse III-Paul Sabatier, Toulouse, France. [2]Institut Universitaire du Cancer de Toulouse IUCT-Oncopole, Toulouse, France. [3]Institut Claudius Regaud, Laboratory of Medical Biology and Oncogenetics, Toulouse, France. [4]Toulouse University Hospital, Toulouse, France. [5]Cancer Research Institute of Montpellier, INSERM U1194, Montpellier University, ICM, Montpellier, France. [6]Unidad de Investigación Clínica de Cáncer de Pulmón, Instituto de Investigación Hospital 12 de Octubre-CNIO, Madrid, Spain. [7]Université Paris-Saclay, Institut Gustave Roussy, Inserm U981, 94800 Villejuif, France

* Contributed equally; # Corresponding authors: favre.gilles@iuct-oncopole.fr; olivier.calvayrac@inserm.fr

Background

Drug-tolerant "dormant" cells (DTC) have emerged as one of the major non-genetic mechanisms driving resistance to targeted therapy (T.T.) in non-small cell lung cancer (NSCLC)[1-4], although the sequence of events leading to entry and exit from dormancy remains poorly described. We recently reported a step-by-step phenotypic and molecular characterization of the different processes involved during the adaptive response to osimertinib in **EGFR-mutant** NSCLC (Figarol *et al.* bioRxiv 2022)[5], and we extended our findings to other oncogenic settings such as **KRAS-** and **BRAF-mutant** or **ALK-translocated** tumor cells treated with their corresponding T.T. We identified of a common non-genetic path of drug adaptation though a pseudo-normal alveolar type 1 differentiation process, which invariably involved Rho/ROCK-dependent actin cytoskeleton remodeling. Among a panel of Rho/ROCK pathway inhibitors, we identified the farnesyltransferase inhibitor (FTi) **tipifarnib** as the most efficient compound in preventing relapse to targeted therapies in EGFR-mutant lung cancer cells, but also in KRAS-mutant and ALK-translocated NSCLC or BRAF-mutant melanoma.

Methods

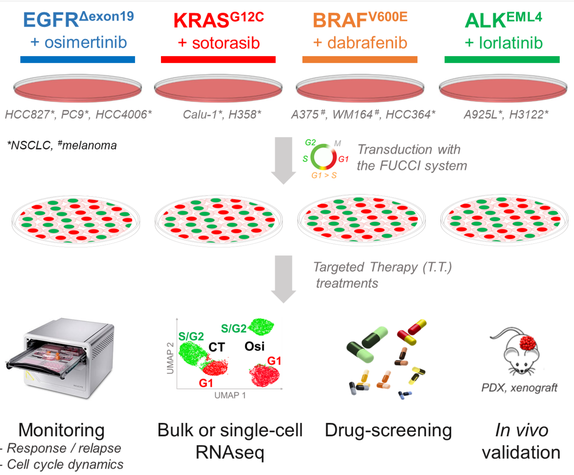

We transduced a panel of oncogene-addicted tumor cells harboring different oncogenic drivers (*i.e.* EGFR, KRAS, BRAF, ALK) with the FUCCI (fluorescence ubiquitination cell cycle indicator) system, and we monitored cell cycle dynamics in response to their corresponding targeted therapies (*i.e. EGFR:* osimertinib, KRAS: sotorasib, BRAF: dabrafenib, ALK-EML4: lorlatinib). We performed bulk and single-cell RNAseq experiments at different time points during the acquisition of resistances in EGFR-mutant NSCLC cell lines, and we compare the transcriptomes with public available data generated in other oncogenic settings. Finally, we performed *in vitro* drug screening to target the most relevant identified pathway of drug-tolerance and we validated the combination in vivo using dedicated NSCLC xenografts and PDX (Patient-Derived Xenografts).

Conclusions

We report that adaptive response to targeted therapy (*T.T.*) in NSCLC is a highly dynamic process which invariably involves dedifferentiation through an alveolar type-1 phenotype with contractile features. Using a screen of Rho/ROCK pathway inhibitors, we found that tipifarnib, a clinically active farnesyltransferase inhibitor, efficiently and durably prevented relapse to *T.T.* in several oncogene-addicted tumors *in vitro* and displayed potent antitumor efficacy *in vivo* with no evidence of toxicity in mice. Collectively, our data strongly support clinical exploration of tipifarnib in combination with *T.T.* to effectively and durably prevent relapse.

Results

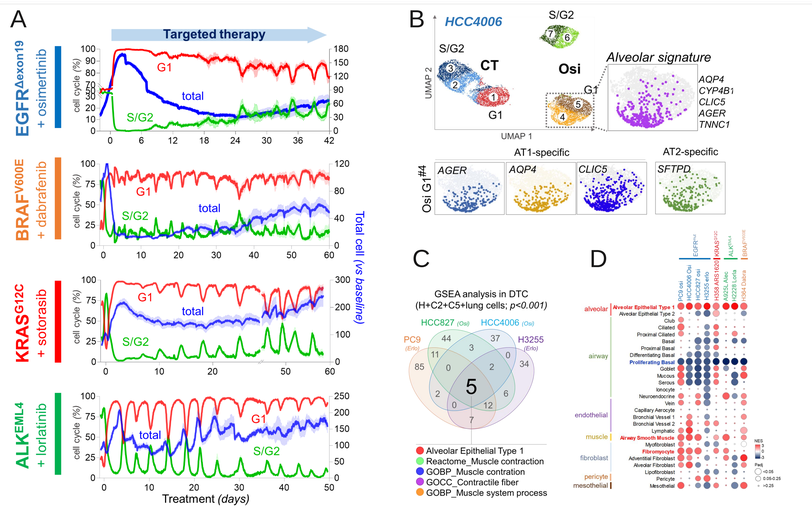

Figure 1. Drug-tolerance is a highly dynamic state that invariably involves an alveolar-like differentiation process

A. Percentage of total cells (blue), S/G2 (green) or G1 (red) populations of EGFR$^{\Delta exon19}$ (HCC4006, blue), BRAF^{V600E} (A375, orange), KRAS^{G12C} (Calu-1, red), and ALK^{EML4} (H3122, green) cell lines, treated with respectively osimertinib (1µM), dabrafenib (1µM), sotorasib (1µM) and lorlatinib (1µM). **B.** UMAP representation of the different populations of untreated and osimertinib-treated HCC4006 cells. The alveolar-like signature is highlighted. **C.** Venn diagram comparing the significantly enriched pathways (GSEA, *p<0.001*) in EGFR-TKI erlotinib- or osimertinib-derived drug-tolerant cells. **D.** Normalized enrichment score (NES) and *p*-value of the different lung signatures during drug-tolerance in several oncogene-addicted tumor cells treated with their corresponding targeted therapy (Osi: Osimertinib [EGFRi]; Alec: Alectinib [ALKi]; Lorla: Lorlatinib [ALKi]; Dabra: Dabrafenib [BRAFi]).

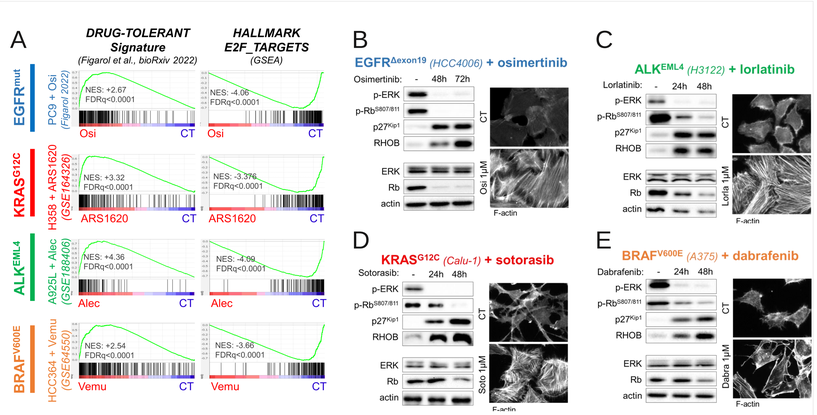

Figure 2. Drug-tolerant cells invariably display cytoskeletal remodeling and Rho/ROCK pathway activation

A. Gene Set Enrichment Analysis (GSEA) analysis using Drug-Tolerant-Signature (Figarol *et al.* bioRxiv 2022)[5] and E2F_targets (GSEA) signatures shows similarities amongst several oncogene-addicted cell lines treated with their corresponding targeted therapy (ARS1620 [KRASG12Ci]; Osi: Osimertinib [EGFRi]; Alec: Alectinib [ALKi]; Vemu: Vemurafenib [BRAFi]). **B-E.** Western blot analysis of phospho-ERK, phospho-Rb, p27 and RHOB levels at the indicated times (left) and phalloidin staining after 10 days of treatment. **B**: HCC4006 cells treated with osimertinib 1µM; **C**: H3122 cells treated with lorlatinib (1µM); **D**: Calu-1 treated with sotorasib (1µM); **E**: A375 cells treated with dabrafenib (1µM).

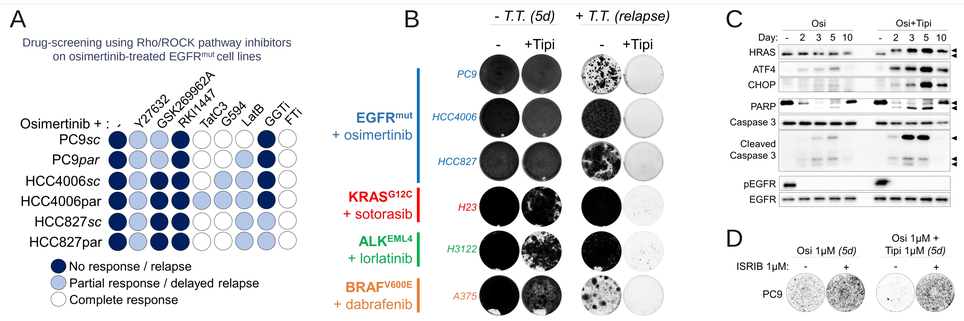

Figure 3. Tipifarnib prevents relapse to targeted therapies by inducing an integrated stress response (ISR)-mediated apoptotic pathway

A. Drug screening of Rho/ROCK inhibitors in combination with 1µM osimertinib in EGFR-mutant NSCLC. Deep blue: no response/relapse, light blue: partial/delayed response, white: complete response. **B.** Crystal violet staining of EGFR-mutant (blue), KRAS-mutant (red), ALK-translocated (green) and BRAF-mutant (orange) cell lines treated with their corresponding targeted therapy (*T.T.*) until relapse, alone or in combination with tipifarnib (1µM). Osimertinib, sotorasib, lorlatinib and dabrafenib were used at 1µM. **C.** Protein expression by Western blot of ATF4, CHOP, HRAS, PARP, total and cleaved caspase 3, total and pEGFR in response to osimertinib (1µM) or osimertinib (1µM) + tipifarnib (1µM). **D.** Cristal violet staining of PC9 cells pre-treated or not for 24h with integrated stress response inhibitor (ISRIB, 1µM) and treated for 5 days with 1µM osimertinib alone or in combination with 1µM tipifanib.

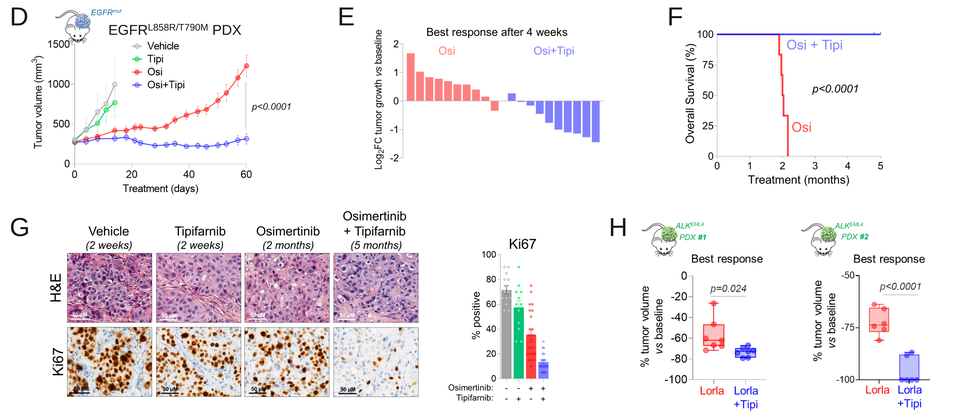

Figure 4. Tipifarnib prevents relapse to targeted therapies *in vivo*

A. Mean tumor volume of PC9 xenografts treated 5 d/w with vehicle (n=6), tipifarnib (Tipi, 80mg/kg, *b.i.d.*; n=6), osimertinib (Osi, 5 mg/kg, *q.d.*; n=10), or by the combo (Osi + Tipi; n=12). Graph represents mean ± SEM. **B.** Change in tumor volume versus baseline of PC9 xenografts after 6 months of treatment with osimertinib or a combination of osimertinib + tipifarnib. **C.** Progression-free survival (PFS) of PC9 xenografted mice treated with osimertinib or osimertinib + tipifarnib. *P*-value was determined by log-rank Mantel-Cox test. **D.** Mean tumor volume of a PDX model of EGFR$^{L858R/T790M}$ NSCLC treated 5 d/w with vehicle (n=4), tipifarnib (Tipi, 80mg/kg, *b.i.d.*; n=5), osimertinib (Osi, 5 mg/kg, *q.d.*; n=10), or by the combo (Osi + Tipi; n=10). Graph represents mean ± SEM. **E.** Log2 fold change of the PDX growth compared to baseline after 60 days of treatment with osimertinib or osimertinib+tipifarnib. **F.** Overall survival (OS) of EGFR$^{L858R/T790M}$ PDX mice treated with osimertinib or osimertinib + tipifarnib. The graph is the result of one cohort of mice with n = 6 mice in both arms. *P*-value was determined by log-rank Mantel-Cox test. **G.** Left: Representative images of Hematoxylin and Eosin (H&E) (top) and Ki67 (bottom) IHC stainings of PDX tumors collected after 2 weeks, 2 months and 5 months of treatment with tipifarnib, osimertinib, and osimertinib + tipifarnib, respectively. Right: Quantification of Ki67 IHC scores. **H.** Percentage ot tumor regression at the time of best response in two different ALK-ELM4 NSCLC PDX models treated with lorlatinib (Lorla, 30 mg/kg, *q.d*) or in combination with tipifarnib ((Tipi, 80mg/kg, *b.i.d*).

References **1.** Sharma *et al.*, Cell, 2010; **2.** Hata *et al.* Nat Med, 2016; **3.** Ramirez *et al.*, Nat Comm, 2016; **4.** Kurppa *et al.*, Cancer Cell, 2020; **5.** Figarol *et al.*, bioRxiv, 2022 (doi.org/10.1101/2022.04.01.486707)

Fundings Part of this study received financial support from Kura Oncology, Inc. through a sponsored research contract